Citation for the published Journal paper:
Title:
Auxiliary beam terrain-scattered interference suppression: reflection system and radar performance

Author:
Svante Björklund, Anders Nelander, Mats Pettersson

Journal:
IET Radar, Sonar & Navigation

Year:
2013
Vol.
7
Issue:
8
Pagination:
836-847
URL/DOI to the paper:
10.1049/iet-rsn.2011.0407

Auxiliary Beam Terrain Scattered Interference Suppression - Reflection System and Radar Performance

Svante Björklund[1], Anders Nelander[2], Mats I. Pettersson[3]

[12]Swedish Defence Research Agency (FOI), P.O. Box 1165, SE-581 11 Linköping, Sweden
[13]Blekinge Institute of Technology, SE-371 79 Karlskrona, Sweden
[1]svabj@foi.se, [2]andnel@foi.se, [3]mtp@bth.se

ABSTRACT

Terrain-scattered interference (TSI), i.e. jammer signals reflected on the earth's surface, is a significant problem to military airborne radar. In auxiliary beam TSI suppression the TSI in the main radar beam is estimated by a single or several auxiliary beams and is subtracted from the main beam channel. The signal to subtract is the auxiliary beam signals fed through an estimate of the "reflection system", which describes the scattering on the surface.

We first present results on the structure of this TSI suppression, on the estimation of the reflection system and on the quality of the estimate. We then derive theoretical expressions for the SINR (Signal to Interference plus Noise Ratio) and the remaining TSI power for a single auxiliary beam. Since the SINR is directly connected to the radar performance, we can see what factors affect the performance and how. We notice that when the estimated reflection system is missing one or more delays of the true system, the TSI filter cannot suppress the TSI signal completely. This phenomenon, which we call "TSI leakage", has a very large impact on the performance. The SINR cannot be kept constant. Instead, an "SINR improvement" can be defined.

1 INTRODUCTION

Terrain-scattered interference (TSI) or *hot clutter* are signals from jammers which are reflected on the ground or sea before they are received by a radar. In the mainbeam an often weak target signal has to compete with TSI. TSI is a significant problem to military airborne radar systems and should be suppressed.

Several approaches to suppress TSI are proposed in the literature. Low sidelobes [5], adaptive beamforming and sidelobe cancellation (SLC) [9] are suggested to be used against TSI in the sidelobes. Fast-time STAP (space-time adaptive processing) [11, 13, 21, 22, 28] is proposed to be used against TSI in the mainbeam. Fast-time means range bin to range bin sampling. It does not mean fast execution. In cases where both monostatic (normal) clutter and TSI exist, the monostatic clutter is suggested to be suppressed either separately before [28] or after [13, 28] the TSI suppression or together with the TSI by 3D STAP [13, 15]. All three approaches have advantages and drawbacks [13, 28]. Some of the literature about TSI suppression is not widely accessible. After year 2005 we have found nearly nothing published about TSI suppression.

Fast-time TSI suppression methods for TSI in the mainbeam are usually of one of two different architectures [13], either the *auxiliary beam* architecture (also called *sidelobe canceller* [13]*)*, where the TSI signal in the main radar channel is subtracted by an estimated TSI signal from a single or multiple auxiliary channels, or the *fully adaptive array* (also called *2D STAP* [13] or *Direct Form Processor* [15]), where all antenna channels are processed together.

In the auxiliary beam architecture, the TSI signal in the main radar channel is generated by a *reflection system* with the transmitted jammer signal as input. This system is created by scatterers on the ground or sea with different time delays and directions of arrival. In the fully adaptive array there is no explicit reflection system, since there are no special main and auxiliary channels.

This article consists of two parts. In the first part (Section 2-3) we utilize results from the field of "system identification" [25] and present a new way to view the auxiliary beam architecture which is centred around the reflection system. We model the reflection system by a linear regression and employ least squares to estimate it, which both are well-known theories. By describing the reflection system as a linear regression we can include both structures of the auxiliary beam architecture, namely *single auxiliary beam* and *multiple auxiliary beam*, in the same framework and we can choose which time delays and channels to include in the model of the reflection system. By the least squares theory and extensions by us we get theoretical expressions for the quality of the estimate of the reflection system. These quality expressions can be interesting by themselves but will become really interesting in the second part (Section 4-6), where we use them in our derivation of theoretical expressions for the remaining TSI power after suppression and resulting SINR (Signal to Interference plus Noise Ratio) for a single auxiliary beam when using estimated reflection systems. We can see what factors affect the SINR and how they do it. It is well-known that the SINR is directly related to the radar performance in the form of probability of detection, detection range and estimation accuracy. There the advantages with our new way of viewing the auxiliary beam architecture are realized.

We will see that our use of the reflection system is equivalent to the ubiquitous SMI (Sample Matrix Inversion) method in the STAP and adaptive beamforming literature, which makes our results widely applicable for auxiliary beam TSI suppression.

Some of our results in Section 2-3 are taken from our conference paper [3] but we have extended them with much new material. For instance, paper [3] only treated the single auxiliary beam structure. Some material in [3] is removed here. The results in Section 4-6 are all new and not published before.

Probably the best survey of TSI suppression methods is the article [13]. That article also describes single and multiple auxiliary beam TSI suppression in a general form, but using the STAP SMI approach, which is different from ours. It does not have any derivations of the suppression methods but that can be found in other literature. Furthermore, it does not model the reflection system and does not contain quality expressions. The article [13] assumes that all delays are used, i.e. there are no holes in the delay sequence. Finally, the article [13] does not consider noise in the auxiliary channels.

In [15] an expression for the optimal SINR in the single auxiliary beam is given but only for a known reflection system. Neither it is stated where the receiver noise enters, which makes a comparison with our results more difficult. A classical result for the SINR loss as a function of the number of estimation data and model order for the fully adaptive array when using estimated interference properties is presented in [29]. It cannot be used directly for our problem since the architectures of the suppression methods are different. The result in [29] also assumes the data to have a certain and known probability distribution (Gaussian). Our results are not restricted to that.

In Section 2 we describe the two structures of auxiliary beam TSI suppression, viz. the single auxiliary beam and multiple auxiliary beam structures, and fit both these structures into a general structure. Section 3 treats the estimation of the reflection system, including theoretical expressions for the quality of the estimate. Then in Section 4 we derive the theoretical expressions for TSI power and SINR. We validate that theory with simulations in Section 5. In Section 6 we have a discussion and finally in Section 7 we give some conclusions.

Vectors are denoted by bold lower case letters, matrices by bold upper case letters. Complex conjugate of a quantity b is denoted by b^*, transpose of a matrix $\boldsymbol{B}$ by $\boldsymbol{B}^T$, and complex conjugate transpose by $\boldsymbol{B}^H$.

2 AUXILIARY BEAM TSI SUPPRESSION METHODS

This section describes the auxiliary beam TSI suppression architecture. Section 2.1 presents a general structure for this architecture, which is then specialized to the single auxiliary beam and multiple auxiliary beam cases in Section 2.2 and 2.3. By the general structure and the specializations we will realize that the estimation methods and the properties of the estimated reflection system in Section 3 are valid for both the single and multiple auxiliary beam structures.

2.1 General structure

Auxiliary beam TSI suppression can be depicted by the block diagram in Fig. 1. The principle is to estimate and remove the TSI signal $r(t)$ in the radar main channel signal $m(t)$, where we look for the target. We utilize one or several auxiliary radar beams directed towards the jammer or towards the TSI in other directions than the main beam in order to estimate the TSI signal in the main beam. Since we employ a signal which is both spatial from an array antenna and temporal in fast-time, the suppression method belongs to the fast-time STAP group.

The received radar signal in the main channel is (see Fig. 1)

$$\begin{aligned} m(t) &= \boldsymbol{B}_M(\boldsymbol{r}_M(t) + \boldsymbol{s}_M(t) + \boldsymbol{n}_M(t)) = \boldsymbol{B}_M(\boldsymbol{r}_M(t) + \boldsymbol{e}_M(t)) \\ &= r(t) + e(t) \end{aligned} \quad . \tag{1}$$

where $\boldsymbol{r}_M(t)$ are the TSI signals, $\boldsymbol{s}_M(t)$ is the reflected radar signal from targets and (normal) clutter, $\boldsymbol{n}_M(t)$ is the receiver noise in the antenna channels used for the main channel and $\boldsymbol{e}_M(t) = \boldsymbol{s}_M(t) + \boldsymbol{n}_M(t)$. The block $\boldsymbol{B}_M$ is the main channel beamformer. The signals $r(t) = \boldsymbol{B}_M\boldsymbol{r}_M(t)$ and $e(t) = \boldsymbol{B}_M\boldsymbol{e}_M(t)$ are the TSI signal and "noise" in the main channel. The subscript M is used for the main channel and A for the auxiliary channels.

The block $\boldsymbol{H}_M(q)$ in Fig. 1 is a reflection system from the transmitted jammer signal $\boldsymbol{d}(t)$ to the main channel antenna elements. In the auxiliary channels, $\boldsymbol{H}_A(q)$ and $\boldsymbol{B}_A$ are reflection system and beamformer, respectively, and $\boldsymbol{v}_A(t)$ is receiver noise plus any remaining interference (jammer and radar signal).

The beamformers $\boldsymbol{B}_M$ and $\boldsymbol{B}_A$ are static (i.e. memory-less) linear systems with spatial signals as input and output. These systems can be represented by matrices. Compare with the blocks "$\mathbf{s}$" and "B" in Fig. 3a in [15]. The systems $\boldsymbol{H}_M(q)$, $\boldsymbol{H}_A(q)$, $\boldsymbol{H}_{MA}(q)$ and $\hat{\boldsymbol{H}}_{MA}(q)$ (see below) are linear dynamic systems in fast-time. The input and output signal vectors are spatial. The beamformers $\boldsymbol{B}_M$ and $\boldsymbol{B}_A$ are chosen by us and are therefore known, while the systems $\boldsymbol{H}_M(q)$ and $\boldsymbol{H}_A(q)$ are unknown.

The system $\boldsymbol{H}_{MA}(q)$ such that

$$\boldsymbol{H}_{MA}(q)\boldsymbol{B}_A\boldsymbol{H}_A(q) = \boldsymbol{B}_M\boldsymbol{H}_M(q) \tag{2}$$

is what we call *the reflection system*. If we estimate $\hat{\boldsymbol{H}}_{MA}(q)$ such that

$$\hat{\boldsymbol{H}}_{MA}(q)\boldsymbol{B}_A\boldsymbol{H}_A(q) = \boldsymbol{B}_M\boldsymbol{H}_M(q), \tag{3}$$

then the TSI in the main channel can be cancelled perfectly.

2.2 Single auxiliary beam

In the *single beam structure*, only a single auxiliary beam is used to estimate the TSI signal. The beam is aimed directly towards the jammer, while placing a null in the main beam direction. We assume that the auxiliary beam can measure the direct jammer signal perfectly, giving $\boldsymbol{B}_A\boldsymbol{H}_A(q) = 1$ (a scalar) and $\boldsymbol{a}_A(t) = a(t) = d(t) + v(t)$. The block diagram in Fig. 1 can be simplified to Fig. 2, where $H(q) = \boldsymbol{B}_M\boldsymbol{H}_M(q)$ and $\hat{H}_{MA}(q) = \hat{H}(q)$ with an estimate of the reflection system $H(q)$. The signals are $r(t) = \boldsymbol{B}_M\boldsymbol{r}_M(t)$, $s(t) = \boldsymbol{B}_M\boldsymbol{s}_M(t)$, $n(t) = \boldsymbol{B}_M\boldsymbol{n}_M(t)$ and $v(t) = \boldsymbol{B}_A\boldsymbol{v}_A(t)$.

Other names of this TSI mitigation method is *selected auxiliary TSI mitigation* [13] and *single beam hot clutter canceller* [21]. The method is also said to be treated in some not widely available literature, like [4, 7, 12]. This approach is also a commonly used for noise and interference reduction in time [16] and in space [9, 19].

Note that the processing is conducted in two steps:

(1) Adaptive processing in space: Estimate (in the auxiliary beam) and suppress (in the main beam) the direct jammer signal.

(2) Adaptive processing in time: Suppress the TSI signals in the main channel.

Here we assume a single jammer, $\boldsymbol{d}(t) = d(t)$. If there are several jammers, each jammer has to be suppressed separately. We form an auxiliary beam to each jammer direct signal while nulling the direct signal from the other jammers. For this we need sufficiently many spatial degrees of freedom. After the nulling, the remaining jammer signals in the auxiliary beam can be regarded as noise.

Despite the simple structure of single auxiliary beam TSI suppression, it has some advantages over other suppression methods, see [13, 27, 28]. It also has some drawbacks, see [13, 21].

2.3 Multiple auxiliary beams

In the *multiple beam structure*, also called the *Generalized Sidelobe Canceller* (GLC) method [13, 21], M beams are formed, one of which is the main beam and the other $M - 1$ auxiliary beams must be chosen orthogonal to the main beam to prevent target leakage into the auxiliary channels.

In this structure, Fig. 1 can be simplified to Fig. 3. This block diagram is similar to the one for the single beam structure but with the difference that there are now several spatial channels in the systems and signals in the auxiliary branch. Note that now, $\boldsymbol{B}_A\boldsymbol{H}_A(q) \neq 1$ and $\boldsymbol{a}_A(t) = \boldsymbol{B}_A\boldsymbol{H}_A(q)d(t) + \boldsymbol{v}_{AB}(t)$ with $\boldsymbol{v}_{AB}(t) = \boldsymbol{B}_A\boldsymbol{v}_A(t)$. We again assume a single jammer.

In the multiple beam structure, the reflection system estimate $\hat{\boldsymbol{H}}_{MA}(q)$ should not be an estimate of $H(q) = \boldsymbol{B}_M\boldsymbol{H}_M(q)$ but of $\boldsymbol{H}_{MA}(q)$ in (2). We call $\boldsymbol{H}_{MA}(q)$ the *generalized reflection system*. The signals $r(t)$, $s(t)$, $n(t)$ are as in Section 2.2.

Also in this structure we have the two-step processing in Section 2.2 but now we have several beams in the auxiliary branch to estimate the jammer signal. There are advantages and drawbacks also with the multiple beam structure of auxiliary beam TSI suppression, see [13].

We define a model of the reflection system for the single beam and multiple beam structures of auxiliary beam TSI suppression in Section 3.1. Then, in Section 3.2 we show how the reflection system can be estimated. In Section 3.3 we present theoretical expressions for the quality of the estimated reflection system.

3.1 Model of the reflection system

We model the TSI signal in the main channel $r(t)$ with a linear regression

$$r(t) = \varphi^T(t)\boldsymbol{h} \tag{4}$$

The vector $\varphi^T(t)$ only contains signals $a(t)$ or $a_k(t)$ (see below) and $\boldsymbol{h}$ are the impulse response coefficients in the model of the reflection system $\boldsymbol{H}_{MA}(q)$ with $\boldsymbol{H}_{MA}(q)$ being defined by (2). The elements of $\varphi^T(t)$ are called *regressors*. Since $\varphi^T(t)$ only contains input signals of the system, (4) is an FIR (Finite Impulse Response) system. Other model structures would also be possible, e.g. ARX or Output Error [25]. Especially for the singe beam structure, a FIR model of the reflection system $\boldsymbol{H}_{MA}(q) = H(q)$ is natural because the reflection system can be seen as created by reflections of the transmitted jammer signal at a finite number of point scatterers with different delays.

In the single beam structure, the vector $\varphi^T(t)$ contains the direct jammer signals

$$\varphi^T(t) = [a(t), \ldots, a(t - T_{\mathrm{SA}} + 1)],$$

and

$$\boldsymbol{h} = [h(0), \ldots, h(T_{\mathrm{SA}} - 1)]^T, \tag{5}$$

where T_{SA} is the maximum time delay for this structure.

In the multiple beam structure the vector $\varphi^T(t)$ contains the received jammer signals in the $M-1$ auxiliary channels:

$$\varphi^T(t) = [a_1(t), \ldots, a_1(t - T_{\mathrm{GLC}} + 1), \ldots, a_{M-1}(t), \ldots \\ , a_{M-1}(t - T_{\mathrm{GLC}} + 1)],$$

where $a_i(t)$ is the signal in the i^{th} auxiliary channel at fast time t and T_{GLC} is the maximum time delay for this structure. Here, the impulse response $\boldsymbol{h}$ of the system $\boldsymbol{H}_{MA}(q)$ (2) is:

$$\boldsymbol{h} = [h_1(0), \ldots, h_1(T_{\text{GLC}}-1), \ldots$$
$$h_{M-1}(0), \ldots, h_{M-1}(T_{\text{GLC}}-1)],$$

where $h_i(\tau)$ are the coefficients for the i^{th} auxiliary channel at fast time delay τ.

The number of coefficients in $\boldsymbol{h}$ is $n = T_{\text{SA}}$ for the single beam structure and $n = T_{\text{GLC}}(M-1)$ for the multiple beam structure if there are no "holes" in the possible sequence of coefficients. Note, that it is not necessary that the coefficients are consecutive in time and antenna channels. There may be "holes" in the sequence. We may keep the most important coefficients (the most important scatterers), discard the other and get a better estimate of the reflection system. This is a problem in itself. It is related to *compressed sensing/sampling* [6]. See [24, 25, 26] for general information on how to choose regressors/coefficients. We will see in Section 5.3 that the choice of proper coefficients is important for the radar performance.

3.2 Estimation of the reflection system

There are several methods in the literature to estimate a system like the reflection system without the noise $\boldsymbol{v}_A(t)$ in the auxiliary channels. In [3] we saw that the Least Squares (LS) method [20] and the Prediction Error Method (PEM) [25], well-known in the field of *System Identification*, are equivalent for this system. The Wiener filter, which minimizes the Minimum Mean Square Error (MMSE) [17], can also be employed for the reflection system estimation [21]. Compared to the PEM/LS method, the Wiener/MMSE filter uses ideal ensemble mean values instead of averages of measured data. The ensemble mean values must be estimated and natural choices are the averages used in the PEM/LS method. Then the PEM, LS, Wiener and MMSE methods will give exactly the same estimator of the reflection system. Therefore the expressions for the quality of the estimated reflection system in Section 3.3 will be valid for all these methods.

We will here show how the reflection system can be estimated with the (deterministic) LS (Least Squares) [20]. We can write equation (1) in a different way:

$$\boldsymbol{m}(t_0) = \boldsymbol{r}(t_0) + \boldsymbol{e}(t_0) \tag{6}$$

and the estimate of the TSI signal

$$\hat{\boldsymbol{r}}(t_0) = \boldsymbol{A}(t_0)\hat{\boldsymbol{h}},$$

where $\boldsymbol{m}(t_0) = [m(t_0), \ldots, m(t_0+N-1)]^T$, $\boldsymbol{r}(t_0) = [r(t_0), \ldots, r(t_0+N-1)]^T$, $\boldsymbol{e}(t_0) = [e(t_0), \ldots, e(t_0+N-1)]^T$,

$\hat{\boldsymbol{r}}(t_0) = [\hat{r}(t_0), \ldots, \hat{r}(t_0+N-1)]^T$ and

$$A(t_0) = \begin{bmatrix} \varphi^T(t_0) \\ \vdots \\ \varphi^T(t_0 + n - 1) \\ \vdots \\ \varphi^T(t_0 + N - 1) \end{bmatrix} \tag{7}$$

In equation (6)-(7) the time index t_0 indicates the point of time when the estimation is performed. In the following, t_0 will be omitted in order to simplify the notation. The quantity N is the number of *estimation data* or *identification data*. The estimation data consists of $a(t)$ or $a_k(t)$ in $\boldsymbol{A}$ and of $m(t)$ in $\boldsymbol{m}$.

The estimation problem is with this notation for both the single and multiple beam structures

$$\hat{\boldsymbol{h}} = \arg\min_{\boldsymbol{h}} V_N(\boldsymbol{h}) \tag{8}$$

with the loss function $V_N(\boldsymbol{h})$

$$V_N(\boldsymbol{h}) = \|\boldsymbol{m} - \hat{\boldsymbol{m}}\|^2, \tag{9}$$

where $\|\cdot\|$ denotes the Euclidean norm of a vector. Without radar returns in the main channel we choose $\hat{\boldsymbol{m}} = \hat{\boldsymbol{r}} = \boldsymbol{A}\hat{\boldsymbol{h}}$

Equation (8) has the solution

$$\hat{\boldsymbol{h}} = \arg\min_{\boldsymbol{h}} V_N(\boldsymbol{h}) = (\boldsymbol{A}^H\boldsymbol{A})^{-1}\boldsymbol{A}^H\mathbf{m}. \tag{10}$$

If we define $N \cdot \boldsymbol{f}_N = \boldsymbol{A}^H\boldsymbol{m}$ and $N \cdot \boldsymbol{R}_N = \boldsymbol{A}^H\boldsymbol{A}$, i.e.

$$\boldsymbol{f}_N = \frac{1}{N}\sum_{t=0}^{N-1}\varphi^*(t)m(t) \text{ and } \boldsymbol{R}_N = \frac{1}{N}\sum_{t=0}^{N-1}\varphi^*(t)\varphi^T(t), \tag{11}$$

we can write the solution (10) as

$$\hat{\boldsymbol{h}} = \boldsymbol{R}_N^{-1}\boldsymbol{f}_N. \tag{12}$$

Wee see that this is also the PEM estimate [25]. Furthermore, we realize the matrix $\boldsymbol{R}_N$ is the sample matrix estimate of the ubiquitous interference covariance matrix in adaptive beamforming and STAP [13, 15]. Thus equation (12) is the usual SMI (sample matrix inversion) filter weights of the sidelobe canceller architecture of adaptive beamforming and STAP [13, 15]. This means that our results apply to the usual adaptive beamforming and STAP filter.

We now generalize the LS estimation to the weighted least squares problem (WLS) by introducing the weighting matrix $\boldsymbol{W}$:

$$\hat{\boldsymbol{h}} = \arg\min_{\boldsymbol{h}} V_N(\boldsymbol{h}) \tag{13}$$

with the loss function $V_N(\boldsymbol{h})$ now using a weighted norm

$$\begin{aligned} V_N(\boldsymbol{h}) &= \|\boldsymbol{m} - \hat{\boldsymbol{m}}\|_W^2 = \|\boldsymbol{m} - \boldsymbol{A}\boldsymbol{h}\|_W^2 \\ &= (\boldsymbol{m} - \boldsymbol{A}\boldsymbol{h})^H \boldsymbol{W} (\boldsymbol{m} - \boldsymbol{A}\boldsymbol{h}) \end{aligned} \tag{14}$$

and with the solution [20]

$$\hat{\boldsymbol{h}} = \arg\min_{\boldsymbol{h}} V_N(\boldsymbol{h}) = (\boldsymbol{A}^H \boldsymbol{W} \boldsymbol{A})^{-1} \boldsymbol{A}^H \boldsymbol{W} \boldsymbol{m} \tag{15}$$

if $(\boldsymbol{A}^H \boldsymbol{W} \boldsymbol{A})$ is invertible. With $\boldsymbol{W} = \boldsymbol{I}$ the solution (15) is the same as the unweighted LS solution (10).

The weighting matrix $\boldsymbol{W}$ in WLS is useful when the noise $\boldsymbol{e}$ is not white. The noise $\boldsymbol{e}$ could be non-white when the target is distributed or the clutter is correlated, both cases when the radar resolution is high. By choosing the weighting matrix as

$$\boldsymbol{W} = (\boldsymbol{R}_{\boldsymbol{e}}^*)^{-1} \tag{16}$$

with $\boldsymbol{R}_{\boldsymbol{e}} = \mathrm{E}\{(\boldsymbol{e} - \mathrm{E}\{\boldsymbol{e}\})^* (\boldsymbol{e} - \mathrm{E}\{\boldsymbol{e}\})^T\}$ we achieve the smallest variance of the estimate $\hat{\boldsymbol{h}}$. This can be realized by using the Gauss-Markov Theorem in [20] and our definition of the covariance matrix in calculations similar to the ones in [20]. This estimate $\hat{\boldsymbol{h}}$ is called the *best linear unbiased estimate* (BLUE), the *minimum variance unbiased estimator* (MVUE) or the *Markov estimate.* See also [25].

If the noise $v(t)$ in the auxiliary channels is not negligible, an approach is to use TLS (Total Least Squares) [18, 20]. In [10], LS and TLS were compared in three radar applications for "cancellation of electromagnetic noise-like interference in modern radar systems". TLS gave better performance in two of the applications and LS in one. TLS was less robust than LS and required more computations. The conclusion was that LS is the preferred choice. In our application, the single auxiliary beam structure might cope better with the noise $v(t)$ in the auxiliary channel than the multiple beam structure because the jammer signal is stronger compared to the noise. Therefore LS could be appropriate for single beam and TLS for multiple beam TSI suppression.

Important aspects on employing auxiliary beam TSI suppression is the point of time to estimate the reflection system, the point of time to apply the estimate and what estimation data to choose. Since the TSI is non-stationary, the reflection system must be updated regularly, typically once for each PRI (Pulse Repetition Interval) [13, 28]. The application of the system estimate should be as close as possible in time to the estimation data and the estimation data should be free of monostatic clutter [13, 28]. The single beam structure might better cope with monostatic clutter and targets in the estimation data because the direct jammer signal is strong in the auxiliary channel due to the beam directly towards the jammer.

We will see in this article that the number of estimation data N should be large for good quality of the estimated reflection system and for good radar performance (SINR). However, if we choose too many estimation data some of them will be outdated because of the non-stationarity of the TSI. This will result in lower performance [28]. See the article [28] for suggestions on how to obtain estimation data and how to apply the suppression filter, i.e. the reflection system.

To cope with large signal dimensions and lack of sufficient estimation data in STAP, rank reduction methods are suggested in the literature. In our auxiliary beam TSI suppression architecture, rank reduction can be performed by a matrix multiplication on the received radar snapshot, see [15]. The beamforming matrix $\boldsymbol{B}_A$ in Fig. 1 may contain a matrix for spatial rank reduction.

3.3 Quality of the estimated reflection system

3.3.1 Bias of the estimate

Assume that the (true) received signal in the main beam is

$$\boldsymbol{m} = \boldsymbol{A}\boldsymbol{h}_0 + \boldsymbol{e}, \tag{17}$$

where the jammer signals in $\boldsymbol{A}$ are deterministic, $\boldsymbol{h}_0$ is the true impulse response of the reflection system and the stochastic vector $\boldsymbol{e} = \boldsymbol{s} + \boldsymbol{n}$ is our “noise” (consists of target and clutter reflections $\boldsymbol{s}$ and the receiver noise $\boldsymbol{n}$). Then, from equation (15) and (17) the WLS estimate of $\boldsymbol{h}$ will be

$$\begin{aligned}\hat{\boldsymbol{h}} &= (\boldsymbol{A}^H\boldsymbol{W}\boldsymbol{A})^{-1}\boldsymbol{A}^H\boldsymbol{W}\boldsymbol{m} = (\boldsymbol{A}^H\boldsymbol{W}\boldsymbol{A})^{-1}\boldsymbol{A}^H\boldsymbol{W}(\boldsymbol{A}\boldsymbol{h}_0 + \boldsymbol{e}) \\ &= \boldsymbol{h}_0 + (\boldsymbol{A}^H\boldsymbol{W}\boldsymbol{A})^{-1}\boldsymbol{A}^H\boldsymbol{W}\boldsymbol{e}\end{aligned} \tag{18}$$

The bias of the estimated impulse response is

$$\begin{aligned}\boldsymbol{b} &= \mathrm{E}\{\hat{\boldsymbol{h}}\} - \boldsymbol{h}_0 = \mathrm{E}\{(\boldsymbol{A}^H\boldsymbol{W}\boldsymbol{A})^{-1}\boldsymbol{A}^H\boldsymbol{W}\boldsymbol{e}\} \\ &= (\boldsymbol{A}^H\boldsymbol{W}\boldsymbol{A})^{-1}\boldsymbol{A}^H\boldsymbol{W}\boldsymbol{m}_e\end{aligned} \tag{19}$$

where $\boldsymbol{m}_e = \mathrm{E}\{\boldsymbol{e}\}$. If the mean value of $\boldsymbol{e}$ is zero, i.e. $\boldsymbol{m}_e = 0$, the bias of the estimate $\hat{\boldsymbol{h}}$ will be zero. This can also be realized using results from system identification by noting that our FIR model $\boldsymbol{m} = \boldsymbol{A}\boldsymbol{h} + \boldsymbol{e}$ is at the same time an OE (Output Error) model [25]. It is known that it is possible to estimate OE models without bias if the true system can be described exactly by the model.

This is valid even if the noise model cannot describe the true noise system. However, this would not be the case if we had general ARX structures [25]. These would not be of the OE structure. See [25] for more information about this. If the mean value of $\boldsymbol{e}$ is not zero, then the bias of the estimate $\hat{\boldsymbol{h}}$ will probably not be zero.

If the criterion is unweighted, i.e. $\boldsymbol{W} = \boldsymbol{I}$, the bias simplifies to

$$\boldsymbol{b} = \frac{1}{N}\boldsymbol{R}_N^{-1}\boldsymbol{A}^H\boldsymbol{m}_{\boldsymbol{e}}. \tag{20}$$

Since $\boldsymbol{A}$ consists of the jammer signal $d(t)$, we get the following:

$$\boldsymbol{b} \propto 1/\sqrt{\lambda_d}, \tag{21}$$

where $\propto$ means "proportional to" and λ_d is the jammer power in the estimation data.

We see from (19), (20) and (21) that the bias depends on the mean value of $\boldsymbol{e}$, the received jammer signals in $\boldsymbol{A}$ (especially the jammer power λ_d), the weighting matrix $\boldsymbol{W}$ and the number of estimation data N. We realize from (18) that the bias is independent of the colour of the noise $e(t)$.

We have performed some simulations to validate the quality expressions for the reflection system. With the ideal radar setup and ideal reflection system in Section 5.1, our theoretical bias and estimated bias (considered the truth) agreed excellently. For the realistic setup and realistic system, the bias agreement was not so good.

3.3.2 Covariance of the estimate

If there is no bias, i.e. $\mathrm{E}\{\hat{\boldsymbol{h}}\} = \boldsymbol{h}_0$, in the estimated coefficients $\hat{\boldsymbol{h}}$, the covariance matrix of $\hat{\boldsymbol{h}}$ is, from equation (18),

$$\begin{aligned}\boldsymbol{P}_N &= \mathrm{Cov}\{\hat{\boldsymbol{h}}\} = \mathrm{E}\{(\hat{\boldsymbol{h}} - \mathrm{E}\{\hat{\boldsymbol{h}}\})^*(\hat{\boldsymbol{h}} - \mathrm{E}\{\hat{\boldsymbol{h}}\})^T\} \\ &= \mathrm{E}\{(\boldsymbol{A}^H\boldsymbol{W}\boldsymbol{A})^{-*}\boldsymbol{A}^T\boldsymbol{W}^*\boldsymbol{e}^*\boldsymbol{e}^T\boldsymbol{W}^T\boldsymbol{A}^*(\boldsymbol{A}^H\boldsymbol{W}\boldsymbol{A})^{-T}\} \\ &= (\boldsymbol{A}^T\boldsymbol{W}^*\boldsymbol{A}^*)^{-1}\boldsymbol{A}^T\boldsymbol{W}^*\boldsymbol{R}_{\boldsymbol{e}}\boldsymbol{W}^T\boldsymbol{A}^*(\boldsymbol{A}^T\boldsymbol{W}^T\boldsymbol{A}^*)^{-1}\end{aligned} \tag{22}$$

If the noise $\boldsymbol{e}$ is white, i.e. its covariance matrix $\boldsymbol{R}_{\boldsymbol{e}} = \lambda_e\boldsymbol{I}$, where λ_e is the power of $e(t)$ in the estimation data, and the criterion is unweighted, i.e. $\boldsymbol{W} = \boldsymbol{I}$, the covariance simplifies to

$$\boldsymbol{P}_N = \lambda_e(\boldsymbol{A}^T\boldsymbol{A}^*)^{-1} = \lambda_e((\boldsymbol{A}^H\boldsymbol{A})^{-1})^* = \frac{1}{N}\lambda_e(\boldsymbol{R}_N^{-1})^*, \tag{23}$$

where $\boldsymbol{R}_N$ is given by equation (11). When we derive the remaining TSI power and SINR after suppression (Section 4.1) we need (23). In [25] similar calculations as here are performed but only for systems with real valued signals. The application of TSI suppression is not treated in [20, 25]. Since $\boldsymbol{A}$ consists of the jammer signal $d(t)$, the following is also valid:

$$\boldsymbol{P}_N \propto 1/(\mathrm{E}\{d^2(t)\}) = 1/\lambda_d, \tag{24}$$

We see, the stronger jammer the better $\hat{\boldsymbol{h}}$.

The true power λ_e of $\boldsymbol{e}$ in (23) is not known but can be estimated. If $\mathrm{E}\{\boldsymbol{e}\} = 0$ and $\boldsymbol{e}$ is white, an unbiased estimate is given by [25]

$$\hat{\lambda}_e = \frac{N}{N-n} V_N(\boldsymbol{h}),$$

where $V_N(\boldsymbol{h})$ is the loss function (9) or (14). Thus an estimate of $\boldsymbol{P}_N$ in the white noise case is

$$\hat{\boldsymbol{P}}_N = \frac{1}{N}\hat{\lambda}_e(\boldsymbol{R}_N^{-1})^*. \tag{25}$$

When the bias of $\hat{\boldsymbol{h}}$ is zero and n and N are large, we have approximately for the variance of the frequency function of the estimated jammer reflection system $\hat{H}(q)$ [25]

$$\mathrm{Var}\{\hat{H}(e^{i\omega}|\boldsymbol{h})\} \approx \frac{n}{N}\frac{\Phi_e(\omega)}{\Phi_d(\omega)}, \tag{26}$$

where $\Phi_e(\omega)$ and $\Phi_d(\omega)$ are the frequency spectra at estimation for $e(t) = s(t) + n(t)$ and $d(t)$, respectively. Here we clearly see that increasing the model order n makes the estimated model worse but increasing the number of estimation data N makes the model better. Increasing the "noise" (target, clutter and receiver noise power) and/or decreasing the jammer signal power at estimation time will make the estimated model worse and vice versa.

3.3.3 Noise in a single auxiliary channel

We now look at what happens for the single auxiliary beam case if we have estimated the reflection system as in Section 3.2, but there is noise present in the auxiliary channel at estimation time, i.e. $v(t) \neq 0$. Then $\hat{\boldsymbol{h}}$ in (12) and (15) will not be optimal but we can still compute the covariance $\boldsymbol{P}_N = \mathrm{Cov}\{\hat{\boldsymbol{h}}\}$. We assume now that $d(t)$ and $v(t)$ are uncorrelated in time and with each other. This assumption should be valid, except perhaps for a repeater jammer, when $d(t)$ might be correlated in time. We have not seen any literature about TSI and its suppression for repeater jammers. Then

$$\boldsymbol{R}_N = \frac{1}{N}\left(\sum_{t=0}^{N-1} \varphi^*(t)\varphi^T(t)\right) \approx (\lambda_d + \lambda_v)\boldsymbol{I}_n \tag{27}$$

where $\lambda_d = \mathrm{E}\{|d(t)^2|\}$ and $\lambda_v = \mathrm{E}\{|v(t)^2|\}$ are the jammer power and auxiliary noise power in the estimation data and $\boldsymbol{I}_n$ is the $n \times n$ identity matrix. If $d(t)$ and $v(t)$ are ergodic processes then $\boldsymbol{R}_N$ will converge to the right side of (27) when $N \to \infty$. For limited N the equation (27) will be an approximation. From (23) and (27) we now get the covariance matrix of the estimated reflection system

$$\boldsymbol{P}_N = \frac{1}{N}\lambda_e(\boldsymbol{R}_N^{-1})^* \approx \frac{1}{N} \cdot \frac{\lambda_e}{\lambda_d + \lambda_v}\boldsymbol{I}_n \tag{28}$$

Here we see how the number of estimation data, the power of jammer, auxiliary channel noise and main channel noise (target, clutter and receiver noise) at the estimation influence the variance of the estimated reflection system. It seems like in (28) that stronger noise in the auxiliary channel at the estimation will give a better estimated system and better TSI suppression. However, the estimated coefficients will probably get a bias because $v(t)$ is a false “jammer signal” which is not present in the main channel. This we have seen by simulations. We will need (28) in Section 4.1.

In our simulations with the ideal radar setup and ideal reflection system in Section 5.1, our theoretical variance and estimated variance (considered the truth) was excellent. For the realistic setup and realistic system, the agreement was rather good. We noted that it is important to take the noise $v(t)$ in the auxiliary channel into account as in (28).

4 THEORY FOR TSI POWER AND SINR

In this section we derive theoretical expressions for the remaining TSI power after suppression and the SINR (Signal to Interference plus Noise Ratio) in the single auxiliary beam structure.

4.1 Remaining TSI power after suppression

First, we derive expressions for the remaining TSI power in the main channel before and after suppression. These quantities are the key quantities from which we can derive other quantities like the SINR.

We model the true reflection system coefficients $h(t)$ as stochastic and the estimated reflection system coefficients $\hat{h}(t)$ as the true coefficients $h(t)$ plus zero mean uncorrelated errors $\varepsilon(t)$:

$$\hat{h}(t) = h(t) + \varepsilon(t)\,. \tag{29}$$

This implies that the bias of the estimated coefficients will be zero (Section 3.3.1) and the vectors $\boldsymbol{h}$ and $\hat{\boldsymbol{h}}$ in (5), (12) and (15) will be stochastic.

The signals $r(t)$ and $\hat{r}(t)$ are then stochastic processes which are statistically dependent on $\boldsymbol{h}$. The powers, expectations and variances which we compute are conditioned on $\boldsymbol{h}$. When we write $\mathrm{V}\{\hat{h}(t)\}$, we mean $\mathrm{V}\{\hat{h}(t)\} = \mathrm{Var}\{\hat{h}(t)|\boldsymbol{h}\}$, which is the variance of the coefficients of the estimated reflection system when $\boldsymbol{h}$ is known. This variance is the diagonal elements of $\boldsymbol{P}_N$ in (22), (23) and (28).

If we assume $d(t)$ is a white process, we can write the TSI power in the main channel without suppression as

$$\begin{aligned}\mathrm{Power}\{r(t)\} &= \mathrm{E}\{|r(t)|^2|\boldsymbol{h}\} = \mathrm{E}\left\{\left|\sum_{\tau=0}^{n-1} h(\tau)d(t-\tau)\right|^2 |\boldsymbol{h}\right\} \\ &= \mathrm{E}\left\{\sum_{\tau=0}^{n-1} |h(\tau)|^2|d(t-\tau)|^2|\boldsymbol{h}\right\} = P_d\sum_{\tau=0}^{n-1}\mathrm{E}\{|h(\tau)|^2|\boldsymbol{h}\} \\ &= P_d\sum_{\tau=0}^{n-1}|h(\tau)|^2 = P_d\|\boldsymbol{h}\|^2\end{aligned} \tag{30}$$

The third equality follows from $d(t)$ being uncorrelated in time. The quantity P_d is the jammer power during TSI suppression filtering. $\|\boldsymbol{h}\|$ is the Euclidean norm of the vector $\boldsymbol{h}$ and is also a measure of the strength of the true reflection system. We see in (30) that the power of $r(t)$ is dependent on the jammer power and the strength of the reflection system, as expected.

Now, we first note that

$$\begin{aligned}\mathrm{V}\{\hat{h}(t)\} &\equiv \mathrm{Var}\{\hat{h}(t)|\boldsymbol{h}\} \\ &= \mathrm{E}\{|\varepsilon(t)|^2|\boldsymbol{h}\} = \mathrm{E}\{|\varepsilon(t)|^2\}\end{aligned}\quad , \tag{31}$$

utilizing (29), the uncorrelation between $h(t)$ and $\varepsilon(t)$ and the zero mean of $\varepsilon(t)$. We observe that the variance of the estimated reflection system is independent of the strength of the true reflection coefficients $|h(t)|$.

Then, if we assume the following: the number of estimated system coefficients is the same as the number of true coefficients ($=n$); the delays are the same in the estimated and the true systems; $d(t)$ and $v(t)$ are white stationary processes in time; $d(t)$, $v(t)$, $h(t)$ and $\varepsilon(t)$ are uncorrelated with each other, we get the power of the remaining TSI signal in the main channel after suppression as (see Appendix A)

$$\mathrm{Power}\{r(t)-\hat{r}(t)\} = (P_d+P_v)\mathrm{Tr}\{\boldsymbol{P}_N\} + P_v\|\boldsymbol{h}\|^2 \tag{32}$$

where P_v is the power of $v(t)$ during TSI suppression filtering, $\boldsymbol{P}_N$ is given in (22), (23) or (28) and $\mathrm{Tr}\{\boldsymbol{B}\}$ is the trace of a square matrix $\boldsymbol{B}$ (= the sum of the diagonal elements). Wee see that, $\mathrm{Power}\{r(t)-\hat{r}(t)\}$ is dependent on the jammer power and auxiliary channel noise power at the TSI suppression, the variance of the estimated coefficients and of the strength of the true system. Note that in the term $P_v\|\boldsymbol{h}\|^2$, P_v belongs to the auxiliary channel and $\|\boldsymbol{h}\|^2$ to the main channel.

The signal $e(t) = s(t)+n(t)$ does not seem to matter for this computation. It is not part of the calculation of the remaining TSI signal or power in (32). However, $e(t)$ matters for the estimation of the reflection system and therefore also for the remaining TSI signal or power, as we will see.

Now, we utilize (28). For limited N this equation is an approximation as noted in Section 3.3.3. For us it is only important that the diagonal elements are sufficiently correct because of the trace operation in (32) which gives with (28)

$$\mathrm{Tr}\{\boldsymbol{P}_N\} \approx \mathrm{Tr}\left\{\frac{1}{N}\cdot\frac{\lambda_e}{\lambda_d+\lambda_v}\boldsymbol{I}_n\right\} = \frac{n}{N}\frac{\lambda_e}{(\lambda_d+\lambda_v)}. \tag{33}$$

If we insert this in (32) we arrive at

$$\mathrm{Power}\{r(t)-\hat{r}(t)\} = (P_d+P_v)\cdot\frac{n}{N}\frac{\lambda_e}{(\lambda_d+\lambda_v)} + P_v\|\boldsymbol{h}\|^2. \tag{34}$$

We see that the remaining TSI power also is dependent on the model order n, the number of estimation data N and signal powers (jammer, auxiliary channel noise and $e(t)$) during the estimation.

It appears in (34) as if a stronger noise in the auxiliary channel at estimation gives a lower TSI power. See Section 3.3.3 for a comment on this.

If $P_d = \lambda_d$ and $P_v = \lambda_v$ then (34) simplifies to

$$\mathrm{Power}\{r(t)-\hat{r}(t)\} = \frac{n}{N}\lambda_e + P_v\|\boldsymbol{h}\|^2, \tag{35}$$

which is independent of the jammer power.

4.2 Signal to Interference plus Noise Ratio

Now, we will derive expressions for the SINR for the single auxiliary beam structure. The SINR is the principal radar performance measure, directly affecting the probability of detection, detection range and estimation accuracy.

The SINR without TSI suppression is, using (30),

$$\mathrm{SINR_{wo}} = \frac{P_s}{\mathrm{Power}\{r(t)\} + P_n} = \frac{P_s}{P_d\|\boldsymbol{h}\|^2 + P_n}, \tag{36}$$

where P_s is the target power and P_n the receiver noise in the main channel at TSI suppression filtering. We assume absence of monostatic clutter at suppression. Such clutter could be handled separately as described in [28]. This SINR is dependent on the jammer power and the strength of the true reflection system.

The SINR with TSI suppression is using (32)

$$\begin{aligned}\mathrm{SINR_w} &= \frac{P_s}{\mathrm{Power}\{r(t) - \hat{r}(t)\} + P_n} \\ &= \frac{P_s}{(P_d + P_v)\mathrm{Tr}\{\boldsymbol{P}_N\} + P_v\|\boldsymbol{h}\|^2 + P_n}\end{aligned} \quad . \tag{37}$$

This SINR is dependent on the jammer power and auxiliary channel noise power during TSI filtering, the variance of the estimated reflection system coefficients and on the strength of the true reflection system.

Using the expression in (34) we also get

$$\mathrm{SINR_w} \approx \frac{P_s}{(P_d + P_v) \cdot \frac{n}{N} \frac{\lambda_e}{(\lambda_d + \lambda_v)} + P_v\|\boldsymbol{h}\|^2 + P_n}. \tag{38}$$

Here we note that the SINR also is dependent on the model order n, the number of estimation data N and the jammer power and auxiliary channel noise power and power of $e(t)$ during the estimation.

With $P_d = \lambda_d$ and $P_v = \lambda_v$ this simplifies to

$$\mathrm{SINR_w} \approx \frac{P_s}{\frac{n}{N}\lambda_e + P_v\|\boldsymbol{h}\|^2 + P_n}, \tag{39}$$

which is independent of jammer power. Thus, the SINR should be able to be independent of the jammer power. The reason is that a stronger jammer at filtering is balanced by a better estimate of the reflection system. We see that when $N \to \infty$, there will still be a SINR loss due to the noise in the auxiliary channel. This is not the case in the expression in [29]. The SINR expressions in [15] show no dependence on the number of estimation data because they assume known TSI properties.

In this section we validate our theory for TSI power and SINR against simulations. We will see that the theory agrees well with the simulations despite the fact that the assumptions for the optimal TSI filter is not completely fulfilled. The exception is when there are missing true delays in the model of the reflection system but we have an explanation for this.

5.1 Simulation setup

The simulation scenarios consist of two parts, definition of the true reflection system and definition of the rest of the scenario. The latter we call the *radar setup*.

In the *ideal radar setup* there is no noise $v(t)$ in the auxiliary channel and no target in the estimation data. In the *realistic radar setup* there is one point target (power 20 dB) at range $N_R/2$ in the estimation data and noise $v(t)$ (zero-mean white complex Gaussian with power 0 dB). The number N_R is the number of range bins.

Four different true reflection systems have been employed. The *ideal system* is a simple reflection system with $n = 10$ complex coefficients with amplitude 0.1 = -20 dB and uncorrelated uniform random phase, see Fig. 4. The (more) *realistic system* has uncorrelated complex gaussian coefficients with delay dependent variance $[0.1\exp(-t/10)]^2$, see Fig. 4. The number of true coefficients is the same as the number of estimation data, which usually is much larger than the number of estimated coefficients. The system '*fullconst+s*', is like the ideal system but has one more coefficient, which is weak (amplitude $0.01 = -40$ dB). The system '*fullconst+1*', is like 'fullconst+s' but the extra coefficient is strong (amplitude $0.1 = -20$ dB).

Especially in wireless communications, reflection systems have been studied, e.g. in [2, 8, 30]. The measurements in [8] are somewhat similar to our ideal system. Our more realistic reflection system does not behave exactly as the measurements in [2, 30] but has a character similar to them. The simulations assume either that no monostatic clutter is present or that it can be suppressed separately (see Section 1).

For both radar setups the noise $n(t)$ in the main channel was zero-mean white complex Gaussian with power 0 dB. Also at suppression filtering there was a point target (power 20 dB) at range $N_R/2$. The jammer power P_d at suppression was either constant at $P_d = \mathrm{E}\{d^2(t)\} = 20$ dB or varied from -20 to +60 dB in steps of 1 dB. In most simulations $\lambda_d = P_d$ but in Section 5.4, λ_d is fixed at $\lambda_d = 20$ dB . There were different random reflection systems for each used number of data N but the same random system was employed for all used different jammer powers P_d. The estimated system was always of FIR structure with $n = 10$ coefficients. The number of Monte Carlo simulations was 100.

We will in the simulation results show two types of graphs. First, we will show graphs of the power of the TSI signal in the main channel without suppression, $r(t)$, and with suppression, $r(t) - \hat{r}(t)$ (also called the *remaining TSI signal*). Both theoretical values according to (30) and (34) and values estimated from the simulations are displayed. This will give four curves in each graph, labelled *Theo r(t)* (30), *Theo8 r(t)-rHat(t)* (34), *Sim r(t)* (estimated, without suppression) and *Sim r(t)-rHat(t)* (estimated, with). See Fig. 5 for an example.

Second, we will show graphs of the SINR without or with TSI suppression. Both theoretical values from (36) and (38) and values estimated from the simulations are displayed. The four curves are labelled *Theo wo.* (36), *Theo8 w.* (38) , *Est wo.* (estimated, without suppression) and *Est w.* (estimated, with). See Fig. 5 for an example.

The values estimated from the simulations are considered the truth in all graphs.

5.2 Results for the ideal and realistic scenario

With the ideal radar setup and the ideal true system the theory agrees very well with the simulations. With the realistic radar setup and the realistic true system the theory for the TSI power and the SINR after suppression only agrees with the simulations for jammer power $P_d \leq 10$ dB (Fig. 5). We will see the reason for the failure in Section 5.3. For the ideal true system the TSI suppression always succeeds in keeping a constant SINR despite an increasing jammer power, which is also predicted by (39). See the "ideal" curve in Fig. 6. For the realistic true system the constant SINR cannot be maintained but we can define a *SINR improvement* as the difference between SINR with TSI suppression and SINR without TSI suppression (Fig. 5).

5.3 Results for missing delays

Fig. 6 shows the TSI signal power as a function of jammer power for different true systems. The realistic radar setup was employed. As a function of jammer power there are different deviations of the theory from the simulation depending on the true system. As a function of number of data, only for the true system 'fullconst+1' the theoretical value of the remaining TSI power differs significantly from the estimated one.

For the ideal true system the estimated system has all delays which are present in the true one and the theory agrees with the simulation. In the true systems 'fullconst+s' and 'fullconst+1' there is an extra delay in the system which is not present in the estimated one. The true system 'fullconst+s' has a small extra coefficients for the extra delay, causing a weak TSI signal to slip into the main channel. The true system 'fullconst+1' has a strong extra coefficient causing a stronger TSI signal to slip in. Since the estimated system does not have a coefficient for the extra delay, it has no chance to cancel this extra TSI signal. We call this phenomenon *TSI leakage* and it can be seen as the disagreement between theory and simulations in Fig. 6.

5.4 Different jammer power for estimation and filtering

Fig. 7 displays what happens if the jammer power is not the same for estimation and filtering. The graph depicts the TSI signal power as a function of the jammer power P_d at the suppression for different true systems while the estimation jammer power is fixed at $\lambda_d = 20$ dB .

For the case without TSI leakage (ideal true system) our theory agrees well with the simulation. Also for the case with small TSI leakage (true system 'fullconst+s') the theory agrees. Only for the true system 'fullconst+1' the theoretical value of the remaining TSI power differs significantly from the estimated one.

6 DISCUSSION ABOUT THE RADAR PERFORMANCE

In the derivations of the theory in Chapter 4 we have utilized a number of assumptions. We have seen that having the correct delays in the estimated reflection system is very important and our theory will fail if this is not the case. The important thing is that the estimated system is not missing delays with strong system coefficients. Compare the result for the systems 'fullconst+s' and 'fullconst+1'. In reality, the true reflection system will most likely not be limited in delay but the impulse response will wear off indefinitely. This would make it impossible to completely cancel the TSI. We will not achieve a constant SINR independent of the jammer power. We will instead get a certain SINR improvement. One way to increase the SINR improvement could be, not to choose the delays in the estimated reflection system consecutively but choose the delays with the strongest true coefficients. See Section 3.1 and the references there. In the opposite case, if we had too many delays in the estimated system, the filter would have the ability to cancel all leaking TSI signals but it also would give a higher variance of the estimated system coefficients, see (26), and therefore lower SINR, equation (38). It will be a trade-off.

It is often suggested in the literature [11, 14, 23], that $R_{\text{ft}} = R_{\text{tsi}}$ for the required number of fast-time taps R_{ft}, where R_{tsi} is the maximum delay of the true reflection system. We have not seen a proof for that. In [1] the condition

$$R_{\text{ft}} > \frac{N_d \cdot (R_{\text{tsi}} - 1)}{L - N_d} \tag{40}$$

for the required number R_{ft} which "guarantees hot-clutter rejectability" for fully adaptive fast-time STAP is given. In (14), L is the number of antenna channels and N_d the number of jammers. Equation (40) is a sufficient but not necessary condition and it does not guarantee the resulting SINR. We can realize from (40) that to some extent there is a trade-off between spatial and temporal DoFs (Degrees of Freedom) in order to suppress the TSI. Using (40) we can also see that the requirements on R_{ft} can be both $R_{\text{ft}} \ll R_{\text{tsi}}$ or $R_{\text{ft}} \gg R_{\text{tsi}}$ depending on the case. In our simulations we have seen that $R_{\text{ft}} \geq R_{\text{tsi}}$ is necessary to avoid TSI leakage, which is in agreement with [11, 14, 23]. But we have no extra spatial DoFs to play with as in (40).

Another assumption to question is whether the jammer transmits white noise. This is a very common assumption and reasonable but we have not investigated what happens for non-white jamming. We have not seen any literature on TSI suppression for non-white jamming. We also assume that the signal $e(t) = s(t) + n(t)$ is white. It is reasonable that the receiver noise $n(t)$ is white. Also a point target in $s(t)$ will have a white spectrum. If the radar range resolution is very high, it could resolve the target into several dependent scatterers and the target signal could be correlated. Also any remaining clutter (part of $e(t)$) could be correlated for high radar resolution.

A fourth assumption to consider is that the number of estimation data should be large. For a 1D filter in fast-time as our TSI filter, the problem is not as large. In a simple simulation our theory gave an error in the theoretical SINR of about 3 dB for $N = n$, 0.7 dB for $N = 2n$, 0.5 dB for $N = 3n$ and 0.3 dB for $N = 4n$.

Yet another assumption is that the bias in the estimated coefficients of the reflection system should be zero in (23), (28) and (29). In Section 3.3.1 we saw that the bias can be zero according to the theory but in the simulations it was not zero. Despite that, our theory for TSI power and SINR agrees with our simulations. The theory is robust to this assumption.

Our expressions for SINR work even if there is a target signal in the estimation data. A target is not allowed to be present [31] for the SINR loss expression in [29].

A derivation of the TSI power and SINR for the multiple beam structure would be more complicated than for a single beam. However, it is probable that the TSI power and SINR for multiple beams should qualitatively behave as the ones for a single beam. The interpretation of $\|\boldsymbol{h}\|^2$ in our TSI power and SINR expressions must be changed since for multiple beams, $\boldsymbol{h}$ are the coefficients of the true system $\boldsymbol{H}_{MA}(q)$ in (2). For the multiple beam structure, (40) tells us that the number of delays need not always be the same in the estimated reflection system and in the true system for good suppression.

7 CONCLUSIONS

7.1 Conclusions for the reflection system (Section 2-3)

We have presented a new way to view auxiliary beam TSI (Terrain Scattered Interference) suppression, centred around the reflection system.

We have put the single beam and multiple beam structures of the auxiliary beam TSI suppression in a common framework.

We see that the reflection system is the same as the usual adaptive filter weights in the well-known SMI (sample matrix inversion) sidelobe canceller of adaptive beamforming and STAP. Our matrix $\boldsymbol{R}_N$ is the sample matrix estimate of the ubiquitous interference covariance matrix. Because of this our results apply also to this usual filter (except (28)).

We present theoretical expressions of the quality (bias and variance) of the estimate of the reflection system and see how some factors influence the quality. The variance expressions are needed when we derive the performance of the radar system.

We have also discussed several other aspects on using auxiliary beam TSI suppression, like only modelling the most important scatterers and estimating with different kinds of noise.

7.2 Conclusions for the radar performance (Section 4-6)

We have studied the radar performance for the single auxiliary beam TSI suppression structure. Our main results are theoretical expressions for remaining TSI power and SINR (Signal to Interference plus Noise Ratio) after suppression filtering, equations (32), (34), (35), (37), (38) and (39). Since the SINR is directly connected to the radar performance, with these expressions, it is possible to see what factors affect the performance and how they do it. Among others we note that ideally the TSI suppression should be able to keep the SINR constant regardless of the jammer power. The TSI power and SINR should also in the multiple auxiliary beam structure qualitatively behave as our theoretical expressions.

In all simulations (single auxiliary beam) where the estimated reflection system has all the delays of the true system the theory agrees very well with the simulations, which are considered the truth. However, when the estimated system is missing one or more delays of the true system, the TSI filter cannot suppress the TSI signal with these delay(s) and TSI power will slip into the main radar channel. This phenomenon, which we call *TSI leakage*, has a very large impact on the performance. The SINR cannot be kept constant. We instead can define an *SINR improvement*. Since, in the multiple auxiliary beam structure, spatial and temporal degrees of freedom can in some extent be traded against each other, this paragraph is not expected to be valid for multiple beams.

REFERENCES

1 Abramovich, Y.I.; Spencer, N.K.; Anderson, S.J.; and Gorokhov, A.Y.: 'Stochastic-constraints method in nonstationary hot-clutter cancellation - Part I: Fundamentals and supervised training applications', *IEEE Transactions on Aerospace and Electronic Systems*, Vol. 34, Issue 4, Oct. 1998, pp. 1271-1292.

2 Ahlin, L., and Zander, J.: 'Principles of Wireless Communications', (Studentlitteratur 1998, ISBN 91-44-00762-0).

3 Björklund, S., and Nelander, A.: 'Theoretical Aspects on a Method for Terrain Scattered Interference Mitigation in Radar', Proceedings of 2005 IEEE International Radar Conference, Arlington, Virginia, USA, 9-12 May 2005, pp. 663-668.

4 Brennan, L. E.: 'Preliminary Results of Hot Clutter Cancellation Tests using WSMR Data', Proc. of 3rd Adaptive Sensor Array Processing Workshop 1995 (ASAP-95), vol. 2, March 1995, pp. 515-537.

5 Bürger, W. K.: 'Sidelobe Forming for Ground Clutter and Jammer Suppression for Airborne Active Array Radar', Proceeedings of IEEE International Symposium on Phased Array Systems and Technology, 2003, Boston, Massachusetts, USA, 14-17 Oct. 2003, pp. 271-276.

6 Candès, E., and Wakin ,M.B.: 'An Introduction to Compressive Sampling', *IEEE Signal Processing Magazine*, March 2008, pp. 21-30.

7 Coutts, S. D.: 'Moutaintop jammer multipath mitigation experiment', Proc. of 2nd Adaptive Sensor Array Processing Workshop, MIT Lincoln Laboratory, 15-17 March 1994, 2, pp. 595-624.

8 Driessen, P. F.: 'Prediction of Multipath Delay Profiles in Mountainous Terrain', *IEEE Journal on Selected Areas in Communications*, vol. 18, no. 3, March 2000, pp. 336-346.

9 Farina, A.: 'Antenna-Based Signal Processing Techniques for Radar Systems', (Artech House 1992, ISBN 0-89006-396-6).

10 Farina, A., Golino, G., and Timmoneri, L.: 'Comparison between LS and TLS in adaptive processing for radar systems', *IEE Proceedings Radar, Sonar and Navigation*, Vol. 150 ,Iss. 1, 2003 , pp. 2-6.

11 Fante, R. L., and Torres, J. A.: 'Cancellation of Diffuse Jammer Multipath by an Airborne Adaptive Radar', *IEEE Transactions on Aerospace and Electronic Systems*, Vol. 31, No. 2, April 1995, pp. 805-820.

12 Gabel, R. A.: 'TSI Mitigation Weight Training Experiments', Proc. of the 3rd ARPA Mountaintop Hot Clutter TIM, 1995, pp. 249-294.

13 Gabel, R. A. , Kogon, S. M., and Rabideau, D. J.: ‘Algoritms for mitigating terrain-scattered interference’, *IEE Electronics & Communication Engineering Journal*, Special Issue on Space-Time Adaptive Processing, Vol. 11, No. 1, February 1999, pp. 49-56.

14 Griffiths, L. J.: ‘Linear Constraints in Hot Clutter Cancellation’, Proceedings of ICASSP International Conference on Acoustics, Speech, and Signal Processing 1996, May 7-10, Atlanta, Georgia, USA, pp. 1181-1184.

15 Guerci, J. R., Goldstein, J. S., and Reed, L. S.: ‘Optimal and Adaptive Reduced-Rank STAP’, *IEEE Transactions on Aerospace and Electronic Systems*, Vol. 36, No. 2, April 2000, pp 647-663.

16 Gustafsson, F.: ‘Adaptive Filtering and Change Detection’, (Wiley 2000, ISBN 0-471-49287-6).

17 Gustafsson F., Ljung L., and Millnert M.: ‘Signal Processing’, (Studentlitteratur 2010, ISBN 9789144058351).

18 Huffel S. V., and Vandewalle J.: ‘The Total Least Squares Problem: Computational Aspects and Analysis’, SIAM 1991, ISBN 0-89871-275-0.

19 Johnson, D. H., and Dudgeon, D. E. : ‘Array Signal Processing. Concepts and Techniques’, (Prentice Hall 1993, ISBN 0-13-048513-6).

20 Kailath, T. , Sayed, A. H, and Hassibi, B.: ‘Linear Estimation’, (Prentice Hall 2000, ISBN 0-13-022464-2).

21 Kogon, S. M., Williams, D. B., and Holder E. J.: ‘Beamspace Techniques for Hot Clutter Cancellation’, Proceedings of IEEE ICASSP International Conference on Acoustics, Speech and Signal Processing, May 7-10, Atlanta, Georgia, USA, 1996, pp. 1177-1180.

22 Kogon, S., William, D., and McClellan, J.: ‘Factored Mitigation of Terrain Scattered Interference and Monostatic Clutter’, Procedings of 30th Asilomar Conference on Signals, Systems, and Computers, 3-6 Nov. 1996, Pacific Grove, CA, USA, pp. 526-530.

23 Kogon, S. M., Williams, D. B., and Holder, E. J.: ‘Exploiting coherent multipath for mainbeam jammer suppression’; *IEE Proceedings Radar, Sonar & Navigation*; Vol. 145, No. 5, October 1998, pp. 303-308.

24 Lind, I.: ‘Regressor and Structure Selection - Uses of ANOVA in System Identification’, PhD. Thesis No. 1012, Linköping University, May 2006.

25 Ljung, L.: ‘System Identification’, (Prentice Hall 1999, ISBN-0-13-656695-2).

26 Ohlsson, H.: ‘Regularization for Sparseness and Smoothness. Applications in System Identification and Signal Processing’, PhD thesis, No. 1351, Linköping University, Sweden 2010.

27 Rabideau, D. J.: 'Modulation of Signals in Rapidly Updated Adaptive Filters: Theory, Mitigation, and Applications', Proceedings of 31th Asilomar Conference on Signals, Systems, and Computers, Pacific Grove, CA, USA, 2-5 Nov. 1997, pp. 1665-1669.

28 Rabideau, D. J.: 'Clutter and Jammer Multipath Cancellation in Airborne Adaptive Radar', *IEEE Transactions on Aerospace and Electronic Systems*, Vol. 36, No. 2, April 2000, pp 565-583.

29 Reed, I. S., Mallett, J. D., and Brennan, L. E.: 'Rapid Convergence Rate in Adaptive Arrays', *IEEE Transactions on Aerospace and Electronic Systems*, Vol. 10, No. 6, November 1974, pp. 853-863.

30 Turkmani, A. M. D., Demery, D. A., and Parsons, J. D.: 'Measurement and modelling of wideband mobile radio channels at 900 MHz', *IEE Proceedings I Communications, Speech and Vision*, Vol. 138 , Issue 5, 1991, pp. 447-457.

31 Ward, J., 'Space-Time Adaptive Processing for Airborne Radar', MIT Lincoln Laboratory, Technical Report 1015, 1994.

APPENDIX A : DERIVATION OF THEORETICAL TSI POWER

We will derive equation (32) for the power of the remaining TSI signal in the main channel after suppression. We start without noise $v(t)$ in the auxiliary channel.

We assume the number of estimated system coefficients is the same as the number of true coefficients ($= n$) and the delays are the same in the estimated and the true systems. The TSI power in the main channel after suppression is

$$\begin{aligned}
P_{r-\hat{r}} &= \text{Power}\{r(t) - \hat{r}(t)\} \qquad (41) \\
&= \mathrm{E}\left\{\left|\sum_{\tau=0}^{n-1} h(\tau)d(t-\tau) - \sum_{\nu=0}^{n-1}[h(\nu)+\varepsilon(\nu)]d(t-\nu)\right|^2 \middle| \boldsymbol{h}\right\} \\
&= \sum_{\tau=0}^{n-1}\sum_{\nu=0}^{n-1} \mathrm{E}\{h^*(\tau)h(\nu)d^*(t-\tau)d(t-\nu)|\boldsymbol{h}\} \\
&- \sum_{\tau=0}^{n-1}\sum_{\nu=0}^{n-1} \mathrm{E}\{h^*(\tau)[h(\nu)+\varepsilon(\nu)]d^*(t-\tau)d(t-\nu)|\boldsymbol{h}\} \\
&- \sum_{\tau=0}^{n-1}\sum_{\nu=0}^{n-1} \mathrm{E}\{[h^*(\tau)+\varepsilon^*(\tau)]h(\nu)d^*(t-\tau)d(t-\nu)|\boldsymbol{h}\} \\
&+ \sum_{\tau=0}^{n-1}\sum_{\nu=0}^{n-1} \mathrm{E}\{[h^*(\tau)+\varepsilon^*(\tau)][h(\nu)+\varepsilon(\nu)]d^*(t-\tau)d(t-\nu)|\boldsymbol{h}\}
\end{aligned}$$

When all terms of the type $[h(\nu) + \varepsilon(\nu)]$ are split into double sums of themselves, we get nine double sums from (41).

If we assume $d(t)$ is uncorrelated with $h(t)$ and $\varepsilon(t)$, then

$$E\{[h^*(\tau)+\varepsilon^*(\tau)][h(\nu)+\varepsilon(\nu)]d^*(t-\tau)d(t-\nu)|\boldsymbol{h}\}$$
$$= E\{[h^*(\tau)+\varepsilon^*(\tau)][h(\nu)+\varepsilon(\nu)]|\boldsymbol{h}\}$$
$$\cdot E\{d^*(t-\tau)d(t-\nu)|\boldsymbol{h}\}$$

and the same for similar terms in (41).

If we assume $d(t)$ is white in time, only terms in the double sums in (41) with $\tau = \nu$ will survive and the double sums become single sums. We also assume $d(t)$ is stationary and independent of $\boldsymbol{h}$. Then, the factors $E\{d^*(t-\tau)d(t-\tau)|\boldsymbol{h}\} = E\{|d(t)|^2\} = P_d$ in (41), where P_d is the jammer power during TSI suppression filtering.

Since $h(t)$ and $\varepsilon(t)$ are uncorrelated

$$E\{[h^*(\tau)+\varepsilon^*(\tau)][h(\tau)+\varepsilon(\tau)]|\boldsymbol{h}\} = E\{h^*(\tau)h(\tau)|\boldsymbol{h}\}$$
$$+ E\{h^*(\tau)\varepsilon(\tau)|\boldsymbol{h}\} + E\{\varepsilon^*(\tau)h(\tau)|\boldsymbol{h}\} + E\{\varepsilon^*(\tau)\varepsilon(\tau)|\boldsymbol{h}\}$$
$$= E\{|h(\tau)|^2|\boldsymbol{h}\} + 0 + 0 + E\{|\varepsilon(\tau)|^2|\boldsymbol{h}\}$$

and the same for similar terms in (41).

Now remains from (41)

$$P_{r-\hat{r}} = P_d\sum_{\tau=0}^{n-1}E\{|h(\tau)|^2|\boldsymbol{h}\} - P_d\sum_{\tau=0}^{n-1}E\{|h(\tau)|^2|\boldsymbol{h}\} \quad . \tag{42}$$
$$- P_d\sum_{\tau=0}^{n-1}E\{|h(\tau)|^2|\boldsymbol{h}\} + P_d\sum_{\tau=0}^{n-1}E\{|h(\tau)|^2|\boldsymbol{h}\}$$
$$+ P_d\sum_{\tau=0}^{n-1}E\{|\varepsilon(\tau)|^2|\boldsymbol{h}\} = P_d\sum_{\tau=0}^{n-1}E\{|\varepsilon(\tau)|^2|\boldsymbol{h}\}$$

Using (31), (42) and the trace operator we arrive at

$$P_{r-\hat{r}} = P_d\sum_{\tau=0}^{n-1}V\{\hat{h}(\tau)\} = P_d\mathrm{Tr}\{\boldsymbol{P}_N\} \tag{43}$$

where $\boldsymbol{P}_N$ is the covariance matrix of $\hat{\boldsymbol{h}}$.

Now we turn to the somewhat more complicated case with noise $v(t)$ in the auxiliary channel.

$$P_{r-\hat{r}} = \mathrm{Power}\{r(t)-\hat{r}(t)\} \tag{44}$$
$$= E\left\{\left|\sum_{\tau=0}^{n-1}h(\tau)d(t-\tau) - \sum_{\nu=0}^{n-1}[h(\nu)+\varepsilon(\nu)][d(t-\nu)+v(t-\nu)]\right|^2|\boldsymbol{h}\right\}$$

While we in (41) only had nine double sums, we in (44) have twenty-five.

If we assume $v(t)$ is a white stationary process in time, $d(t)$ and $h(t)$ are uncorrelated with $v(t)$ and use that $h(t)$ and $\varepsilon(t)$ are uncorrelated, we can see that the new double sums also become single sums and that most of the new sums will be zero. The only new non-zero sums of $P_{r-\hat{r}}$ are

$$\sum_{\tau=0}^{n-1} \mathrm{E}\{|h(\tau)|^2|\boldsymbol{h}\}\mathrm{E}\{|v(t-\tau)|^2|\boldsymbol{h}\} + \sum_{\tau=0}^{n-1} \mathrm{E}\{|\varepsilon(\tau)|^2|\boldsymbol{h}\}\mathrm{E}\{|v(t-\tau)|^2|\boldsymbol{h}\} \tag{45}$$

The factors $\mathrm{E}\{|v(t-\tau)|^2|\boldsymbol{h}\} = \mathrm{E}\{|v(t)|^2|\boldsymbol{h}\} = P_v$ are the power of the noise $v(t)$ during TSI suppression. Using $\mathrm{E}\{|h(\tau)|^2|\boldsymbol{h}\} = |h(\tau)|^2$ and (31) the new terms in (45) will be

$$P_v \sum_{\tau=0}^{n-1} |h(\tau)|^2 + P_v \sum_{\tau=0}^{n-1} \mathrm{V}\{\hat{h}(\tau)\}\ . \tag{46}$$

By adding the new terms in (46) to (43) and using $\|\boldsymbol{h}\|^2 = \sum_{\tau=0}^{n-1} |h(\tau)|^2$ and the trace operator we finally arrive at

$$\begin{aligned} P_{r-\hat{r}} &= (P_d + P_v) \sum_{\tau=0}^{n-1} \mathrm{V}\{\hat{h}(\tau)\} + P_v \sum_{\tau=0}^{n-1} |h(\tau)|^2 \\ &= (P_d + P_v)\mathrm{Tr}\{\boldsymbol{P}_N\} + P_v\|\boldsymbol{h}\|^2 \end{aligned}$$

which is equation (32).

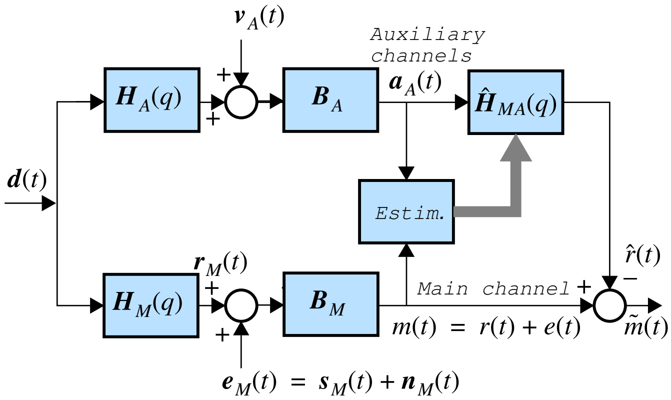

Fig. 1 *Block diagram of auxiliary beam TSI suppression.* $\boldsymbol{d}(t)$ *is the transmitted jammer signal. In the auxiliary channels* $\boldsymbol{v}_A(t)$ *is receiver noise plus remaining interference (jammer and radar signal),* $\boldsymbol{H}_A(q)$ *is the reflection system and* $\boldsymbol{B}_A$ *is the beamformer. In the main channel,* $r(t)$ *is the reflected jammer signals,* $\boldsymbol{H}_M(q)$ *and* $\boldsymbol{B}_M$ *are the reflection system and beamformer,* $\boldsymbol{s}_M(t)$ *is the reflected radar signal from targets and monostatic clutter and* $\boldsymbol{n}_M(t)$ *is the receiver noise.* $\hat{\boldsymbol{H}}_{MA}(q)$ *is the estimated reflection system in (3).*

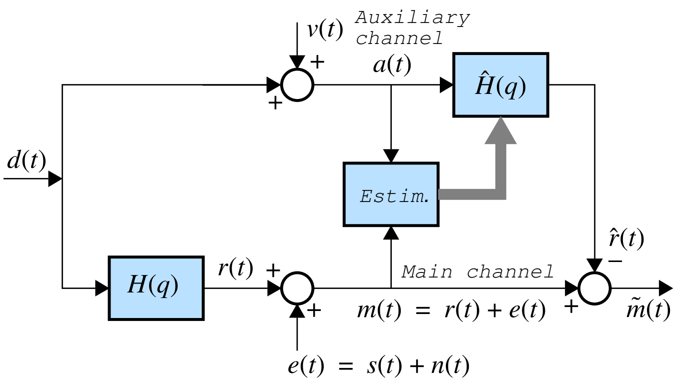

Fig. 2 *Block diagram of single auxiliary beam TSI suppression.* $d(t)$ *is the direct jammer signal.* $v(t)$ *is receiver noise plus remaining interference in the auxiliary channel.* $H(q)$ *is the reflection system and* $r(t)$ *is the TSI (hot clutter),* $s(t)$ *is the reflected radar signal from targets and (normal) clutter and* $n(t)$ *is the receiver noise in the main channel.*

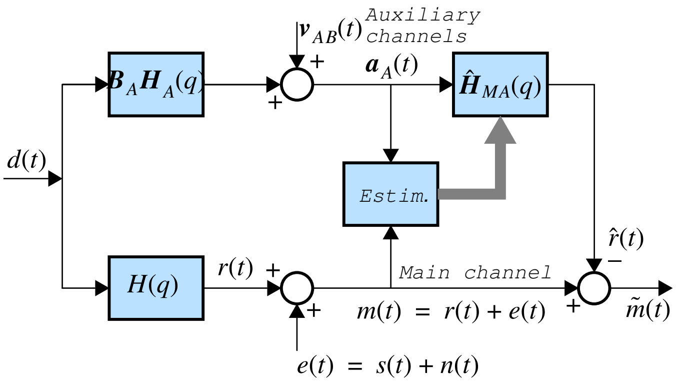

Fig. 3 *Block diagram of multiple auxiliary beam TSI suppression.* $d(t)$ *is the direct jammer signal.* $\mathbf{v}_{AB}(t)$ *is receiver noise plus remaining interference in the auxiliary channel. In the main channel,* $H(q)$ *is the reflection system,* $r(t)$ *is the TSI signal,* $s(t)$ *is the reflected radar signal from targets and monostatic clutter and* $n(t)$ *is the receiver noise.*

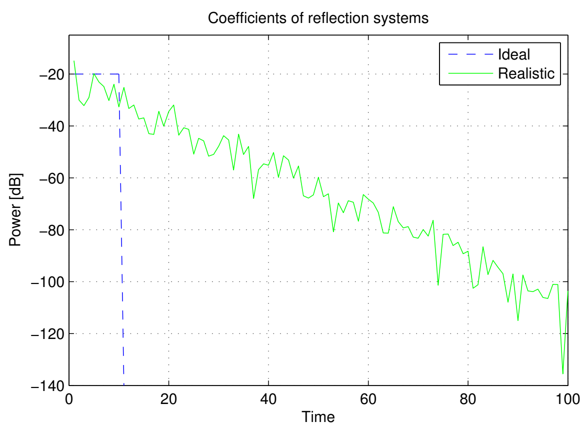

Fig. 4 *Absolute value of the impulse response coefficients of the ideal and realistic system types used in the simulations. Only one realization of the realistic system is shown.*

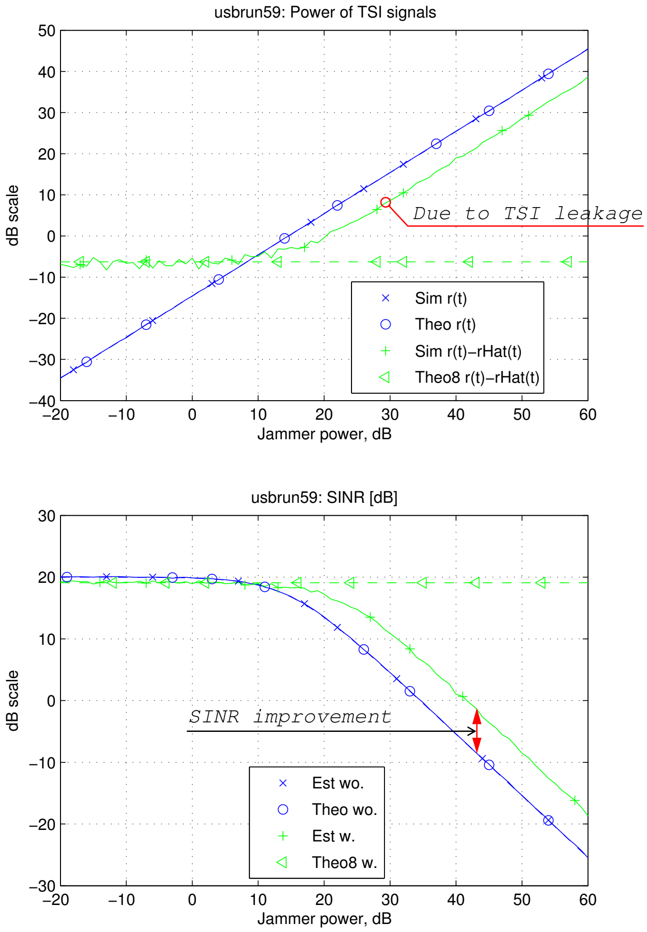

Fig. 5 *Power of TSI signals and SINR as a function of jammer power* $P_d = \lambda_d$. *Realistic radar setup with realistic true system. Top: TSI signal power. Bottom: SINR.*

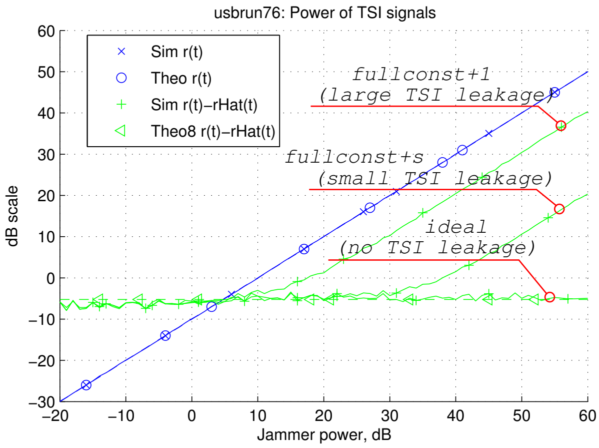

Fig. 6 *Power of TSI signals as a function of jammer power* $P_d = \lambda_d$. *Realistic radar setup.* $N = 100$. *True systems: 'ideal', 'fullconst+s' and 'fullconst+1'.*

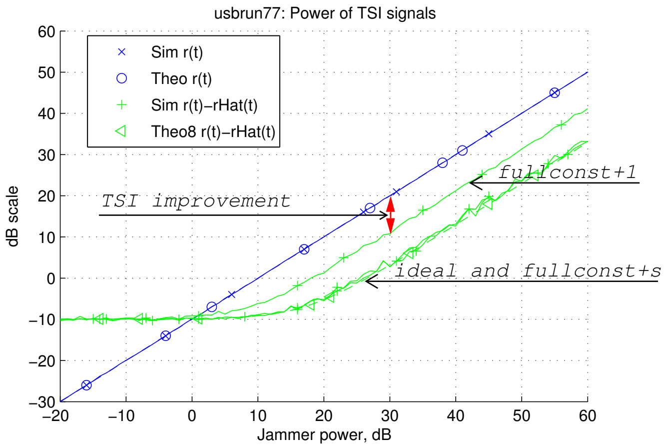

Fig. 7 *Power of TSI signals as a function of jammer power* P_d *at suppression while* $\lambda_d = 20$ dB *is fix. Realistic radar setup. True systems: 'ideal', 'fullconst+s'. and 'fullconst+1'.*

33